3D attitude calculation for the grasper of a crane system with a rotary gyroscope

Xiaolong Zhang, Pauli Mustalahti, Eelis Peltola and Jouni Mattila

***Abstract*——This paper focuses on state calculation for a grasper, which hangs on a heavy-duty machine with rope or links at the boom tip, using a triad-axis rotary gyroscope attached on the grasper. We try to decrease the drift of gyroscope in two direction except the rotation axis. The algorithm was validate on a test bed, which based on a crane system. The test results show that with rotary platform, long-term drift of the gyro decreased and the accuracy of angle integration for the grasper became better.**

Keywords—IMU, quaternion, anti-sway, crane

I. INTRODUCTION

Crane systems are widely used to move loads in factories, forests, construction fields, etc. These systems have a grasper connected to the tip of their manipulator with links or cables, making the grasper not controllable directly since the acceleration from operating the crane and external disturbances move the grasper. To ensure the system's safety and to increase operating efficiency, an anti-sway controller is applied to these cranes to restrict unwanted swaying of the grasper, such as in [1]-[3].

In [1] and [2], the crane grasper swaying is constrained to vertical plane motions, and the sway angle is measured with accuracy sensors directly. [3] presents a grasper rotated around two axes. The hydraulic manipulator has 4 degrees of freedom (DOF), and the state of sway estimation uses two Inertial Measurement Units (IMU), based on an Extended Kalman Filter (EKF) presented in [4].

[4] applied a dynamic model of a grasper system, which hung with multiple links from the boom tip, for fusing the outputs from an accelerometer and gyroscope measuring its sway angle. However, the amplitude of the sway angle in their implementation is relatively small, less than 7 degrees.

In this paper, we develop a measurement approach for a grasper with a rotary gyroscope to be used for anti-sway control. In [5], a rotary IMU is mounted on the wheel of a vehicle and an EKF is applied for fusing the measurements from the IMU's gyroscope and accelerometer together to correct the drift of angular velocity in the rotation axis. A rotary IMU benefits from being easily mountable onto a complete system, unlike encoders. Contrary to [5], in this paper, we do not use a dynamic model and filter, because in our case the dynamic model for a filter is difficult to build. The grasper has three DOF for rotation; the rotation joints experience friction forces and the boom's manipulation frequently adds disturbing acceleration to the grasper. In practical operation, the grasper will hold all kinds of loads with different shapes, which lead to the center of mass changing. In addition, there are other external forces such as wind, the load may collide with other objects, etc. A dynamic model would have to take all of these into account.

We use a triad-axis gyroscope attached to the grasper through a rotary platform. With the rotary gyroscope, measure the angular velocity and integrate the rotation angle of the grasper. The gyroscope rotates with a constant speed respect to the body-fixed frame of the grasper. The gyroscope has less effect with eternal force disturbances, and it is also considered as a reliable sensor in most environments. However, it is well known that the drift of a gyroscope causes the error of angle integration to increase. Even for a high performance, industry-grade gyroscope, the error of angle integration will diverge rapidly without correction by another sensor or frequent calibration. A rotary gyroscope can decrease the drift of measured angular velocity in any axis except the rotation axis.[6], [7] The test results show that our approach is promising, within two minutes the error of the integration for sway angles smaller than 2 degrees.

II. EXPERIMENTAL SETUP

We built the test bed based on a HIAB XS033 crane, as presented in Fig. 1. The hydraulic manipulator has three links and a reach of about 5.3 meters. The lift and tilt joints can rotate in the vertical plane, while the locked base joint has no rotation.

Manuscript received July 15, 2018. This research work was supported in part by the Doctoral School of Industry Innovations (DSII), by Tampere University of Technology (TUT), the Forum for Intelligent Machines (FIMA), and the Academy of Finland (Grant no. 294915).

Xiaolong Zhang is with the Department of Automation and Hydraulic Engineering, Tampere University of Technology, Tampere, FI-33720 Finland (phone: +358449138672; e-mail: xiaolong.zhang@tut.fi).

Pauli Mustalahti is with the Department of Automation and Hydraulic Engineering, Tampere University of Technology, Tampere, FI-33720 Finland (e-mail: pauli.mustalahti@tut.fi).

Eelis Peltola is with the Department of Automation and Hydraulic Engineering, Tampere University of Technology, Tampere, FI-33720 Finland (e-mail: eelis.peltola@tut.fi).

Jouni Mattila is with the Department of Automation and Hydraulic Engineering, Tampere University of Technology, Tampere, FI-33720 Finland (e-mail: jouni.mattila@tut.fi).

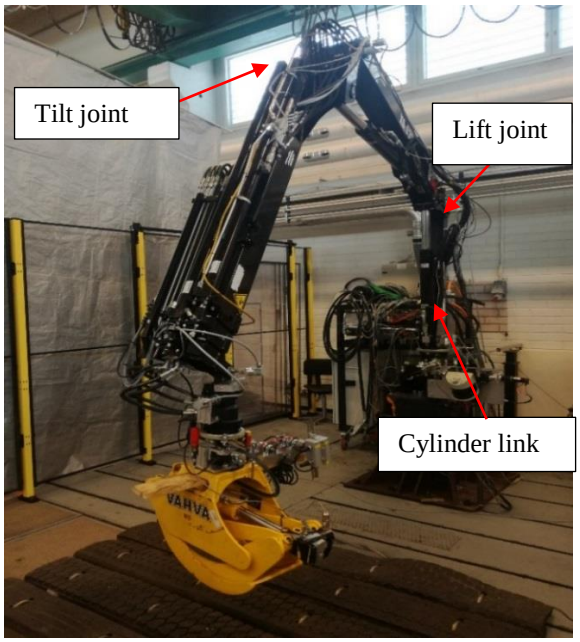

Fig. 1. The HIAB XS033 crane used for test-bed.

Fig. 2 shows the rotation platform attached to the grasper, with the IMU in box rotated by an electric motor; the angular velocity controlled to 250º/s respect by motor controller. Position and velocity references for the rotation of IMU-sensor provide by encoder.

The joints and links, which connect the grasper with the boom tip, are shown in Fig. 3. Position references for the three unactuated joints are also given by encoders.

A CAN-bus connects the sensors to dSpace, and dSpace runs the Simulink model collecting sample data with a rate of 500 Hz/s. The results in this paper were calculated offline with Matlab.

The hardware in the tests summary below:

- PowerPC-based dSpace ds1103 with a sample time of 2 ms
- SICK DFS60B incremental encoder (10000 inc/rev) for the IMU rotation
- Fraba incremental encoders (16384 inc/rev) for the joint 1 and joint 2 angles
- Heidenhain ROD 426 incremental encoder (5000 inc/rev) for the joint 3 angle
- Gripper tool with a mass of 90 kg
- Maxon M110743 motor for rotating the IMU, controlled by an EPOS2 motor controller
- ADIS16485 iSensor MEMS inertial unit by Analog Devices with three-axis angular gyroscope (±450º/s) and three-axis accelerometer (±5g)

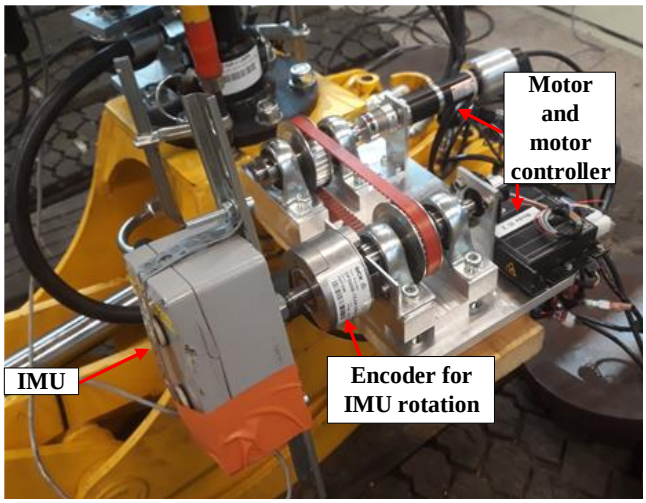

Fig. 2. IMU box and its rotation platform

The IMU in the test bed contains accelerometer; however, our algorithm only uses the gyroscope output.

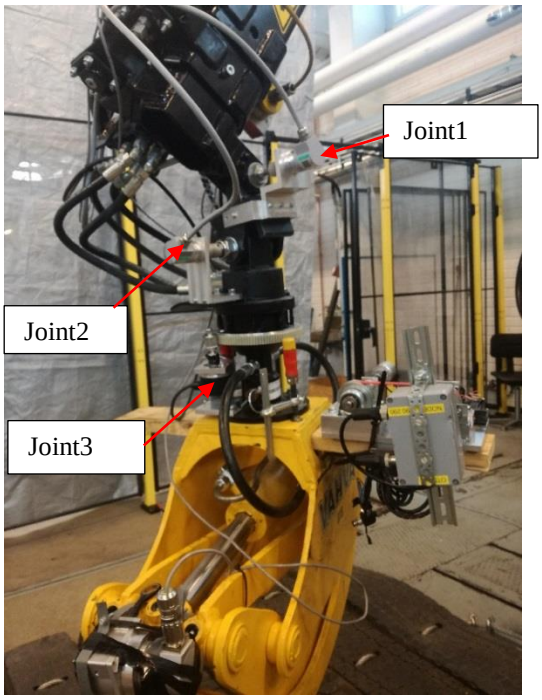

Fig. 3. The unactuated joints and links of grasper

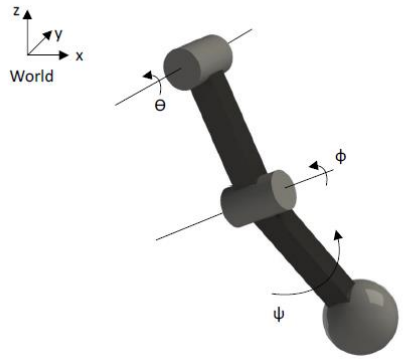

Fig. 4. Model of the system

The grasper system, shown in Fig. 3, may be simplified as a model presented in Fig. 4. The reference of pitch angle Θ in the world frame can attained by combining the output of the encoders of joint 1, the lift joint and tilt joint. The encoder in joint 2 gives the reference for the roll angle φ. However, we cannot lock the base rotation entirely for the cylinder link, indicated in Fig. 1; the reference for roll is not accurate enough. The angle ψ in Fig. 4 corresponds to the joint 3 angle in Fig. 3. Notably, it is not the yaw angle of the grasper in the world frame, as the encoder of joint 3 only gives the rotation angle of the grasper with respect to the body-fixed frame of the link between joints 2 and 3.

Once the link of the grasper is perpendicular to the ground, world frame roughly align with body-fixed frame of the grasper, then the yaw angle coincides with ψ.

III. MATHEMATICAL BACKGROUND

A. Angular Velocity Modulation with a Rotation Gyroscope

Denote the measurements of the gyroscope of the rotation IMU as w_x and w_z, on the x and z axes respectively. Written as true angular rates plus long-term bias and noise:

$$w_x = w_{xt} + b_x + n_x \,, \tag{1}$$

$$w_z = w_{zt} + b_z + n_z \,. \tag{2}$$

Ignoring the noise terms, we transfer these two outputs into the body-fixed frame of the grasper:

$$\dot{\theta}_{bx} = (w_{x_t} + b_x)\cos\emptyset_k - (w_{z_t} + b_z)\sin\emptyset_k \tag{3}$$

$$\dot{\theta}_{bz} = (w_{z_t} + b_z)\cos\emptyset_k + (w_{x_t} + b_x)\sin\emptyset_k \,, \tag{4}$$

where $\emptyset_k$ is the rotation angle of the IMU box. It is the angle of the sensor frame with respect to the body-fixed frame of the grasper, determined by

$$\emptyset_k = \int_0^{t_k} r\, dt \,. \tag{5}$$

In (5), r is the rotation speed of the IMU box. If we assume r is constant and combine (4) and (5), we notice that the integration term that contains the long-term bias will disappear after one complete circle.

In (5), r is the rotation speed of the IMU box. If we assume r is constant and integrate (3) and (4), we notice that the integration term that contains the long-term biases b_x and b_y will disappear after one complete circle.

We set the rotation speed of r in (5) as 250 °/s. The rotation speed of the grasper in each direction is less than 50 °/s for most of the testing time, much smaller than the rotation speed of the gyroscope. Therefore, in our implementation, the majority of angle error caused by long-term bias in two axis directions of the gyroscope can be removed.

For the rotation speed of the grasper in the y-axis of its frame, we use the measurement of gyroscope in this direction minus the angular speed of the IMU box in this direction, which can directly get from the encoder installed with the IMU-box as showing in Fig. 2.

$$\dot{\theta}_{bz} = w_y - r \tag{6}$$

From (3), (4) and (6) we form a virtual gyroscope, which gives the rotation speed of the grasper with respect to the world frame expressed in the body-fixed frame of the grasper.

$$\omega = \begin{bmatrix} \dot{\theta}_{bx} \\ \dot{\theta}_{bz} \\ \dot{\theta}_{bz} \end{bmatrix} \tag{7}$$

B. Angle Integration with Quaternion Form

Since integration of quaternion form for angular velocity is computationally light, and usually the computer of an embedded system has very limited computational resources, we choose quaternion form for expressing rotation.

Defining the rotation quaternion from world frame to local frame in time step k as

$$q_k = \begin{bmatrix} q_1 & q_2 & q_3 & q_4 \end{bmatrix}^T_k \,, \tag{8}$$

the time derivative of q_k becomes

$$\dot{q}_k = \frac{1}{2} q_k \otimes \begin{bmatrix} 0 \\ \omega_k \end{bmatrix} = \frac{1}{2} \Omega(\omega_k) q_k \,, \tag{9}$$

where $\otimes$ denotes quaternion multiplication, ω_k is expressed in the local frame of the grasper in time step k ,which is given by (7), and $\Omega(\omega_k)$ has the form

$$\Omega(\omega)=\begin{bmatrix} 0 & -\omega_x & -\omega_y & -\omega_z \\ \omega_x & 0 & \omega_z & -\omega_y \\ \omega_y & -\omega_z & 0 & \omega_x \\ \omega_z & \omega_y & -\omega_x & 0 \end{bmatrix} . \quad (10)$$

The integration of the rotation quaternion is

$$q_{k+1}=q_k+\dot{q}_k\Delta t\,, \quad (11)$$

where Δt is the sample interval. In addition, (11) is derived based on the Taylor series of $q(t_k+\Delta t)$ around time $t=t_k$, keeping only the first order term. For our implementation, the sample interval is 0.002 seconds. Compare (11) with other complete form, during 3 minutes, the maximum difference is less than 0.15 degree.

The complete integration form is First order integration in [8],

$$q_{k+1}=q_k\otimes\left(q\{\bar{\omega}\Delta t\}+\frac{\Delta t^2}{24}\begin{bmatrix}0\\ \omega_k\times\omega_{k+1}\end{bmatrix}\right) , \quad (12)$$

where

$$\bar{\omega}=\frac{\omega_k+\omega_{k+1}}{2} , \quad (13)$$

and

$$q\{\bar{\omega}\Delta t\}=e^{\bar{\omega}\Delta t}=\begin{bmatrix}\cos(\|\omega\|\Delta t/2)\\ \frac{\omega}{\|\omega\|}\sin(\|\omega\|\Delta t/2)\end{bmatrix}, \quad (14)$$

(12)-(14) is more accuracy than (11), when sample frequency is lower, since it consider angular acceleration and no ignoring of higher order terms. In this paper, the test results is from (11).

We define the initial quaternion as (15), where the frame of the grasper aligns with the world frame:

$$q_0=\begin{bmatrix}1 & 0 & 0 & 0\end{bmatrix}^T \quad (15)$$

In every time step, normalize the quaternion as

$$q_k=\frac{\|q_k\|}{q_k} . \quad (16)$$

The references from encoders in the unactuated joints indicated in Fig. 3 are in the form of Euler angles. Convert the rotation quaternion into Euler angles with (17)-(19):

$$\phi_k=\arctan 2(2(q_{1k}q_{2k}+q_{3k}q_{4k}),\ 1-2(q_{2k}^2+q_{3k}^2)) \quad (17)$$

$$\theta_k=\arcsin(2(q_{1k}q_{3k}+q_{4k}q_{1k})) \quad (18)$$

$${}_w\psi_k=\arctan 2(2(q_{1k}q_{4k}+q_{2k}q_{3k}),\ 1-2(q_{3k}^2+q_{4k}^2)) \quad (19)$$

where $\arctan 2$ is a function that the return value is in four quadrants. q_{k1} to q_{k4} are the elements of quaternion q_k .

${}_w\psi_k$ is given in world frame, however, the reference of joint 3 is expressed in local frame, as shown in Fig. 3 and Fig. 4.

C. Calibration of the Gyroscope

In [6] and [7], a method for calibrating MEMS IMUs is given. For our implementation, if the IMU rotates around the y-axis, ignoring the Earth rotation, a simple error model for the gyroscope is

$$\begin{bmatrix}\delta\omega_x\\ \delta\omega_y\\ \delta\omega_z\end{bmatrix}=\begin{bmatrix}k_{xy}\omega+d_x\\ S_y\omega+d_y\\ k_{zy}\omega+d_z\end{bmatrix} , \quad (20)$$

where d_x, d_y, and d_z are the gyroscope biases in the sensor frame, and $[\delta\omega_x \quad \delta\omega_y \quad \delta\omega_z]^T$ is the error of the gyroscope in the sensor frame. k_{xy} is the factor of the installation error for the x-axis in relation to the y-axis, which means if the y-axis has a rotation speed of ω, because of the installation position inaccuracy it will project into the x-axis an angular speed with that factor. k_{zy} is the factor of the installation error for the z-axis in relation to the y-axis. S_y is the scale factor in the y-axis, indicating the nonlinearity of the gyroscope in this axis, and ω is the rotation speed of the y-axis.

IV. RESULTS

A. Test Procedure

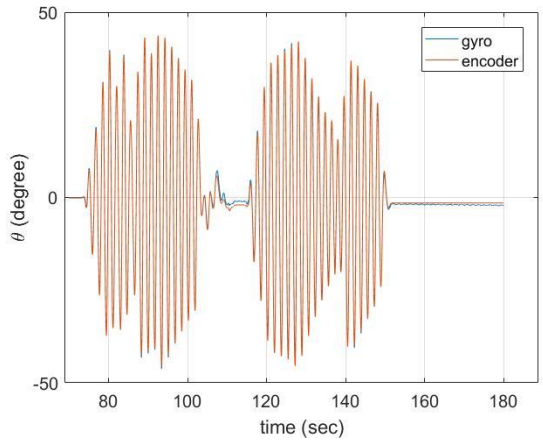

Fig. 5. Pitch angle of the system sway, red line is the reference from encoder, and blue line is from integration of gyroscope.

First, we keep the IMU box and the manipulator stationary for about 30 seconds, take the mean values from the gyroscope's raw output in the x-, y- and z-axes, compare it with zero, and get the bias d_x, d_y and d_z, as defined in (20). Then, only the IMU box is rotated for about 30 seconds, and we take the mean value of the output of gyroscope, with the biases d_x and d_y from the first phase. Using (20), we get k_{xy}, k_{zy} and S_y. From about 70 s, the manipulator is moved frequently, swaying the grasper. During 104 s to 115 s of the test, the sway is manually stopped and the grasper is rotated, simulating external disturbances. At about 151 s, the swaying is manually stopped again, ending the test at 180 s.

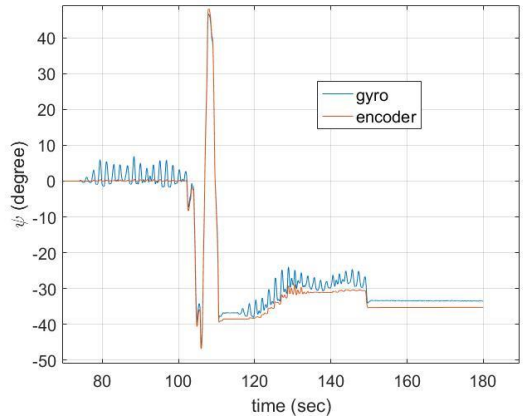

Fig. 6. Rotation of the grasper. The results from the encoder match the reference only during the periods from 104 s to 115 s and 151 s to 180 s.

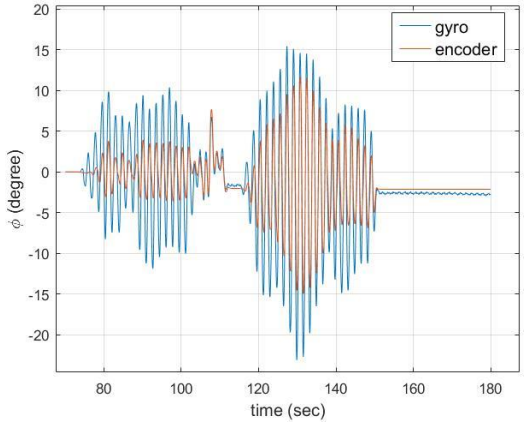

Fig. 7. Roll angle of the system's sway, since the cylinder link of crane has oscillation, the amplitude of gyro's output is bigger than encoder's.

B. Results analysis

Fig. 5 shows the sway in pitch direction; the maximum amplitude is about 45 degrees. The error RMS is 0.831 degrees, and the maximum error is 2.95 degrees at about 127 s. During 104 s to 115 s, θ only has small oscillation, and the curve of integration also follows the reference well, with the error peak being less than 1.8 degrees.

Although the calculation result and the reference for the rotation of grasper present in Fig.6 together, but only during two periods (104 s to 115 s, and 151 s to 180 s), the reference is accuracy, since the world frame coincides with the local frame of joint 3 at these moments, as mentioned in Sec. II and Sec. III.B.

The part of the test from 104 s to 115 s in Fig. 6 is shown enlarged in Fig. 8 The error RMS is 1.43 degrees for this period, while the maximum error is 2.41 degrees and the offset from 110.5 s to 116 s is about 1.7 degrees. During the last period of the test, from 151 s to 180 s, there is also an offset; it is about 1.8 degrees. This offsets may be because of wobble error. In our case, we consider it as the axis of joint rotation is not aligned with the defined axis of the sensor.

As mentioned in Sec. II, the cylinder link of the crane has rotation, so the encoder of joint 2 cannot give an accurate reference in world frame. However, after more than 40 seconds of angle integration, once the boom is kept relatively stationary during 104 s to 115 s, the result of the angle calculation from the gyroscope in roll direction roughly follows the reference curve, and as shown in Fig. 9, the maximum error is less than 2 degrees.

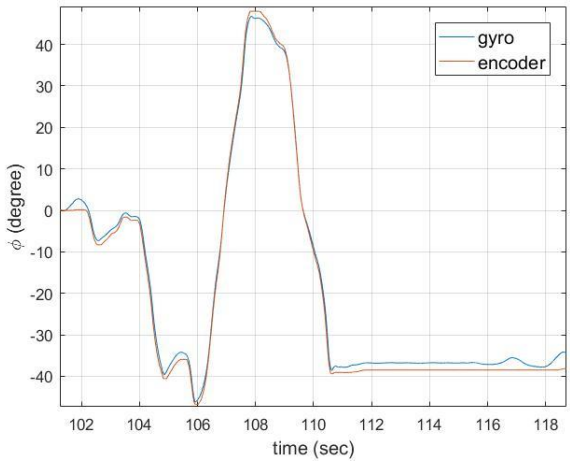

Fig. 8. Yaw rotation of the grasper, with the local frame aligned with the world frame. Enlarged from Fig. 6.

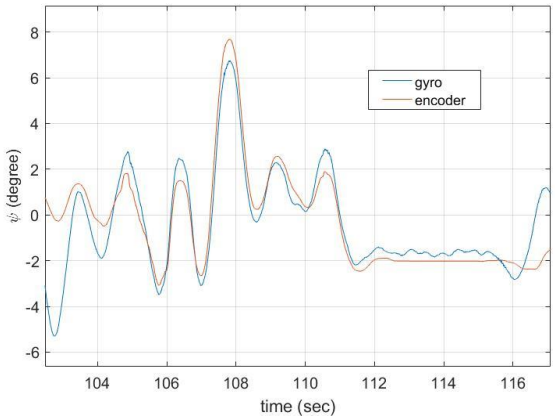

Fig. 9. Sway of the system in roll direction, when the cylinder link of crane has a small rotation angle. Enlarged from Fig. 7.

V. Discussion

As described in Section IV.A, our calibration phase lasts for about 60 seconds. This is because our rotation platform of IMU simply installed on the grasper, the rotation axis of the motor is easily have some changing respect to the gyro's axis. The installation error of the gyro may also slightly change as the temperature varies since the components of devices deforms, but this change is small, and we can count it into the gyro's biases d_x and d_y in (20). In fact, these two biases do not need calibration if we have rough values of the installation error for the two axes, because rotation modulate the long-term of bias, as indicated by (3)-(5), and we use industry-grade gyroscope, the bias is relatively small compared to low-cost gyroscopes. Using the data contain the bias in the two axes only produce some small amplitude oscillation of sine wave in angle integration, if the gyroscope rotate with constant speed. For our implementation, this small sine wave has a small effect; we can notice it from the ending part of the blue lines, in Fig. 5 and Fig. 7.

The raw data of angular velocity is presented in Fig. 10 to show the installation error of the gyro. The rotation platform is kept stationary during data collection. In the beginning, the gyroscope doesn't rotate, and the z-axis output is around zero. Once the gyroscope starts rotating around the y-axis with a velocity of 250 °/sec, the z-axis of the sensor has an output of -4 °/sec, although the rotation platform itself has no rotation with respect to the world frame.

Moreover, once the rotation motor starts, the noise in output from gyroscope increases significantly, and some oscillation is introduced. The introduced noise may be from the electrical motor and the oscillation might result from the center of mass of the IMU not being correctly aligned with the axis of rotation. For a more reliable and higher performance test bed, updating the rotation platform is required.

In the rotation axis of the gyroscope, y-axis, there is no correction method applied to the angular velocity except for the calibration during the beginning. This means that for long-term operation, the integration of the angle will diverge. As discussed above, we may only need to correct the scale factor and bias in the rotation axis. The scale factor of the gyroscope in rotation axis is dependent on temperature, the nonlinearity of the gyroscope in y-axis of the gyroscope, and the installation accuracy between the rotation axis and the sensor axis. Rewrite the second equation of (17) as

$$\begin{aligned} \delta\omega_y &= S_y\omega + d_y \\ &= ({}^{con}S_y + \Delta S_y)\omega + d_y \\ &= {}^{con}S_y\omega + \Delta S_y\omega + d_y \\ &= {}^{con}S_y\omega + \Delta D_y \end{aligned} \quad , \qquad (21)$$

where ${}^{con}S_y$ is fixed to a constant value close to the true value of the scale factor. Moreover, the remaining part of ${}^{con}S_y$, ΔS_y, is absorbed into ΔD_y as the rotation speed of the gyroscope is kept constant. Then, the system only needs to estimate one parameter, ΔD_y. For the data processing, we try setting d_x and d_y as zero, k_{xy} and k_{zy} as constants close to the true value of installation error with some small constant deviation, but for ${}^{con}S_y$ and ΔD_y to give an accurate value, the result of angle output has no significant difference. Only some small oscillating wave is added, which is acceptable for our implementation. However, giving even a small constant disturbance bigger than 0.01 °/sec, the result has an obvious difference of about two degrees for two minutes of angle integration.

Accurately estimating ΔD_y for our system is easy in a stationary case: there is an encoder on the rotation platform, which can give an accurate observation of the varying angle. However, in a dynamic situation, as mentioned in Section I the model is difficult to build, and we may need to introduce other measurement sensors for correcting ΔD_y in the case of long-term operation without interruptions by calibrations of

the gyroscope.

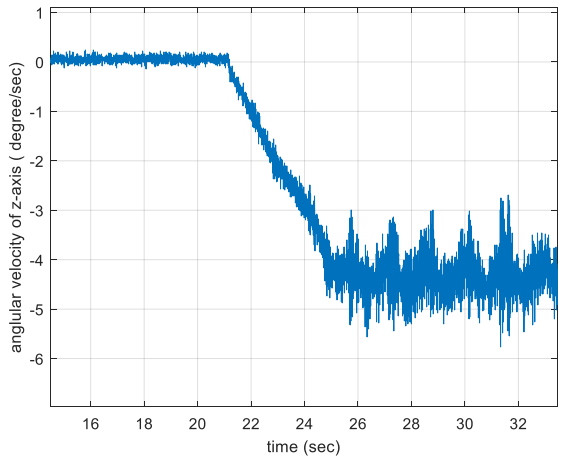

Fig. 10. Raw data from the output of the gyroscope. Once the gyroscope starts rotating, an angular error is projected into other axes.

VI. Future works

The test bed used in this paper is big and cumbersome for the needed task of rotating the gyroscope, and is not practical for real-world use or extensive testing. For future research, the test bed IMU box will be upgraded with a substantially smaller Analog Devices ADIS16475-3 IMU and a built-in rotary unit for the IMU. Fig. 11 shows the unit, containing a motor, an encoder and the rotating IMU connected with a slip ring. This allows us to rotate the IMU only, instead of rotating the complete IMU box. The following key components are added to the setup:

- Hengstler AD35 absolute encoder with length 24 mm and diameter 28 mm
- Six-wire slip ring SRC022-A, with a length of 28 mm and a diameter of 22 mm on the stationary side.
- Maxon DC-max 22 S motor, with length 36 mm and diameter 22 mm, pulse width modulation controlled via an H-bridge by an STM32F4 microcontroller

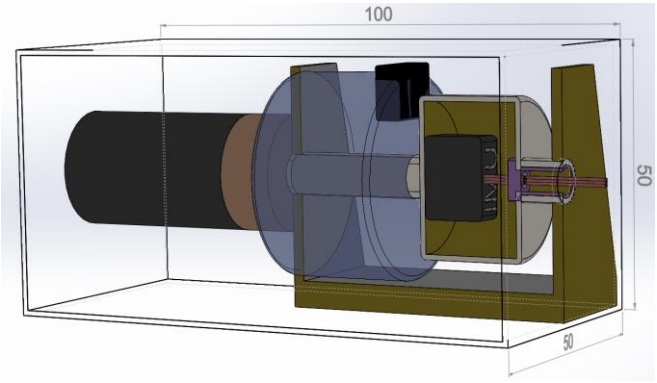

Fig. 11 Sketch of the planned rotary unit, with the motor on the left, encoder in clear blue, and IMU inside a cylinder connected to the slip ring.

The encoder will provide feedback to the microcontroller, which adjusts the speed of the motor to keep the IMU rotating with a steady velocity. The complete electromechanical system fits in an enclosure that is 100 mm long. All signals controlling the motor and reading the encoder and IMU data will be handled by the STM32F4 microcontroller, which sends the data to a real-time computer.

VII. Conclusion

An industry-grade gyroscope with a rotation platform can accurately calculate the attitude of the grasper of the crane. Within two minutes, the RMS error of the attitude is less than two degrees, which allows our method to be applied for anti-sway control in many cases.

Continuously rotating the gyroscope with an external motor can simplify the requirements needed of the angle-calculating algorithm. For long-term operation of the system, the device only need correct one parameters online, which is the bias of angular velocity on the rotation axis.

References

[1] P. Mustalahti and J. Mattila. "Nonlinear full-model-based controller for unactuated joints in vertical plane." *Cybernetics and Intelligent Systems (CIS) and IEEE Conference on Robotics, Automation and Mechatronics (RAM), 2017 IEEE International Conference on*. IEEE, 2017.

[2] Kim, Yong-Seok, Keum-Shik Hong, and Seung-Ki Sul. "Anti-sway control of container cranes: inclinometer, observer, and state feedback." *International Journal of Control, Automation, and Systems* 2.4 (2004): 435-449.

[3] J. Kalmari, J. Backman, and A. Visala. "Nonlinear model predictive control of hydraulic forestry crane with automatic sway damping." *Computers and Electronics in Agriculture* 109 (2014): 36-45.

[4] J. Kalmari, H. Hyyti, and A. Visala. "Sway estimation using inertial measurement units for cranes with a rotating tool." *8th IFAC Symposium on Intelligent Autonomous Vehicles*, Australia, 2013.

[5] X. Zhang, T. Mononen, M. M. Aref, and J. Mattila "Mobile Robotic Spatial Odometry by Low-Cost IMUs" *The 14th IEEE/ASME International Conference on Mechatronic and Embedded Systems and Applications*, Finland, 2018.

[6] S. Du, W. Sun, and Y. Gao, "MEMS IMU error mitigation using rotation modulation technique," *Sensors*, vol. 16, p. 2017, Nov. 2016.

[7] S. Du, "Rotary inertial navigation system with a low-cost MEMS IMU and its integration with GNSS," *Ph.D. dissertation*, Univ. Calgary, 2015.

[8] Sola, Joan. "Quaternion kinematics for the error-state Kalman filter." *arXiv preprint arXiv:1711.02508* (2017).